Development of a numerical correlation for heat transfer coefficients in steam turbines inner chambers

Cite as: AIP Conference Proceedings **2191**, 020067 (2019); https://doi.org/10.1063/1.5138800
Published Online: 17 December 2019

Tommaso Diurno, Matteo Poggiali, Lorenzo Mazzei, et al.

Development of a Numerical Correlation for Heat Transfer Coefficients in Steam Turbines Inner Chambers

Tommaso Diurno[1, a)], Matteo Poggiali[1], Lorenzo Mazzei[1], Antonio Andreini[1], Bruno Facchini[1] and Gabriele Girezzi[2]

[1]*Department of Industrial Engineering, University of Florence, Via S. Marta 3, Firenze – 50139, Italy.*
[2]*Baker Hughes, a GE Company, Via Felice Matteucci 2, Firenze – 50127, Italy.*

[a)] Corresponding author: tommaso.diurno@htc.unifi.it

Abstract. Nowadays, the growing need for advanced solutions to limit the environmental impact in thermal power generation has given rise to significant changes in steam turbines design and operability. In this context, improvement in efficiency and more flexibility in different operating conditions are the major challenges. An increased flexibility is related to rapid load changes, fast start-up and frequent shutdown that could lead to high material thermal stresses in the unit. Hence, in order to achieve the rise in efficiency and to preserve the lifetime of the turbine, a detailed knowledge of the thermal behavior of the turbine is required.
This work is focused on the investigation of flow and heat transfer phenomena in the steam chambers between stator blade carriers. Correlative 1D models are usually used in the industrial practice to estimate heat transfer coefficients to be used as boundary conditions in detailed FEM simulation of the Whole Engine Modelling (WEM). However, the flow pattern in this chamber is complex and this approach could represent an oversimplification, therefore computational fluid dynamic (CFD) analyses have been performed with the aim to obtain a more accurate estimation. All the analyses have been carried out with ANSYS CFX with a quasi-2D axis-symmetric approach. This methodology, despite the need for some simplifications and assumptions to reduce the problem from 3D to quasi-2D, ensures less expensive simulations in terms of computational resources when compared to a fully 3D.
After a numerical setup validation in terms of mesh sensitivity, a parametric CAD has been generated and tested. The goal is to analyze how geometrical parameters (such as the axial distance between the stator blade carriers or the height of the chamber) of the chamber will influence heat transfer coefficients, considering different operating conditions. A design of experiment (DOE) with ANSYS Workbench platform has been carried out in order to perform automatically a set of simulations. Finally, the results obtained have been post-processed to extract a sufficiently accurate correlation for the average Nusselt number applicable for almost all the steam chambers in the turbine even in different operating conditions.

INTRODUCTION

In the last few years, the growing interest in renewable energy has led to radical changes in the power generation sector. In this scenario, the steam turbines are experiencing significant adjustments in the design practice. Specifically, the major changes concern an increase in efficiency, more compact design and more flexibility in different operating condition. The latter is mainly related to the wide use of steam turbine as thermal engine in renewable energy plants, such as in concentrating solar power plants where the fluctuating nature of the solar supply leads to rapid load changes, fast start-up and frequent shutdown. These transient operating conditions could lead to high material stresses and consequently, a detailed knowledge of the thermal behavior of the machine is fundamental in order to preserve the lifetime of the turbine. This, in the industrial practice, is often achieved by using FEM simulations, in which the heat transfer between steam and turbine is modeled by the imposition of a heat transfer coefficients as thermal loads for the solid domain resolution.

However, in most cases, the heat transfer coefficient is calculated with analytical correlations available in literature that resulting in a lack of accuracy when applied at real geometry and in off-design operating conditions. In this regard, the side spaces between stator blade carriers, illustrated in FIGURE 1, are particularly critical areas. Indeed, the flow pattern in this zone is complex and it significantly influences the heat transfer between steam and the wall of the chamber. In these zones, the application of the correlations found in the literature could lead to an excessive simplification. The state of art of flow and heat transfer phenomena in stationary cavities is full of experimental and numerical investigations [1-11], however, since most of these are limited to simple geometry their findings are not accurate enough to correctly predict the flow field and heat transfer coefficients in real steam turbines chambers.

74th ATI National Congress
AIP Conf. Proc. 2191, 020067-1–020067-10; https://doi.org/10.1063/1.5138800
Published by AIP Publishing. 978-0-7354-1938-4/$30.00

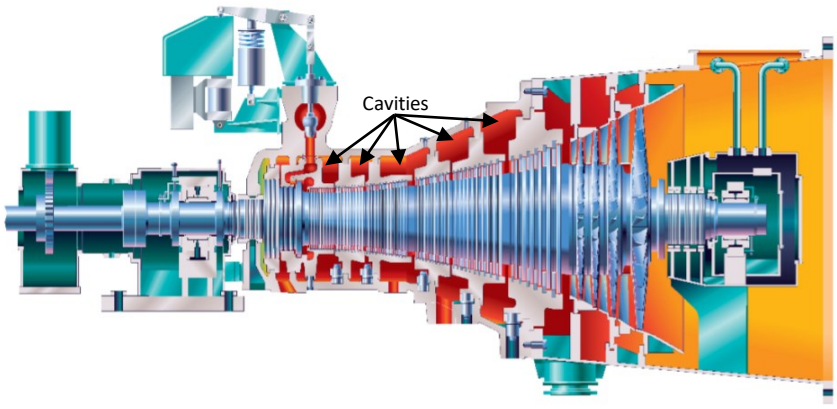

FIGURE 1 – SC axial exhaust steam turbine cross section (BHGE industrial steam turbine). © 2019 Baker Hughes, a GE company, LLC - All rights reserved

More complex cavities (T-shape ad L-shape) have been investigated by A. Aroussi [12-14] with both experiments and numerical simulations, however, the focus of these studies is limited to the flow field and no information about heat transfer is provided.

Recently, Spura et al. [15-16] have performed a series of both experimental and numerical analysis with the aim to improve knowledge about heat transfer in steam turbine cavities with complex geometry. The influence of geometrical parameters on heat transfer coefficients distribution have been evaluated, however, all experimental tests have been carried out with dry air as working fluid.

In the present work, in order to further increase the knowledge about these cavities, a Design of Experiment has been performed with the aim to investigate how geometrical parameters together with thermodynamic conditions of the steam in main flow path influence the heat transfer in the chamber.

Finally, the results of numerical simulations have been processed to extract a correlation for the heat transfer coefficients applicable for almost all the steam chamber in different operating conditions. This correlation could be very useful for the design practice in the early phase of the development process of the turbine to predict in a sufficiently accurate way the thermal loads on the wall structures of the chamber to be used as boundary condition for the FEM model.

NUMERICAL METHODS

Geometry

The geometry object of this study is representative of a standard side space enclosed between stator blade carriers. Due to the modular design of steam turbines, there are many of these cavities along with the entire turbine with similar geometry. Usually, their cross-section presents a T-shape. A schematic view of a steam chamber is reported in FIGURE 2.

The Design of Experiment has been conducted by varying the external diameter (D), the width of the chamber (L1) and the width of the gap (L2). Since the external diameter is directly related to the size of the turbine, by analyzing the available dimensions of the steam turbines manufactured by Baker Hughes, a GE Company (BHGE), four values of D have been chosen to obtain a comprehensive set of geometries.

For each one of the selected external diameters, four characteristic different chamber widths have been chosen. Finally, the width of the gap, which connects the main flow path to the chamber, has been defined as a ratio of L1. L1 and L2 value have been chosen to be representative of the real geometry of the turbines. The total number of geometries simulated is 64.

A comprehensive overview of the dimensions of all geometries generated is reported in TABLE 1.

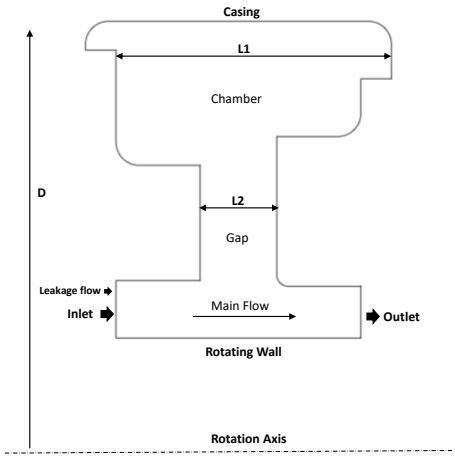

FIGURE 2 - Sketch and nomenclature of the cavity.

D [mm]	250	400	500	630
L1 [mm]	175	265	400	600
L2 [mm]	$\frac{L1}{40}$	$\frac{L1}{16}$	$\frac{L1}{8}$	$\frac{L1}{4}$

TABLE 1 - Geometrical dimensions.

Simulation Setup

The DOE procedure has been implemented by using ANSYS Workbench to automatically perform the set of steady-state CFD RANS simulations solved with commercial 3D Navier-Stokes solver ANSYS® CFX.

The fluid is modeled as dry steam with the IAPWS-IF97 based library by which the thermal and physical properties of the steam are defined as a function of temperature and pressure. The turbulence of flow is modelled with shear stress transport turbulence model (SST) [17] and the advection fluxes of continuity, momentum and total energy equations are calculated with a high-resolution scheme, essentially a second order bounded scheme, while a first order scheme has been used for the convective terms of turbulence equations. Since the focus of the investigation is only on the forced convection heat transfer phenomena the effect of the gravity has been neglected.

For the spatial discretization, a tetrahedral mesh grid is used with a local mesh refinement in the gap and in the chamber to increase the accuracy of flow field resolution in this area where the greatest gradients are expected. The correct resolution of the flow in the boundary layer, a crucial issue for an accurate estimate of the heat transfer between fluid and wall structures, is ensured by the imposition of twenty prismatic elements in order to obtain a dimensionless wall distance y+ around 1.

The dependence of the results on the mesh used has been checked. This has been accomplished by generating five different grids with different element size. The results of the grid sensitivity analysis are reported in FIGURE 3 where the ratio between average HTC calculated on casing surface and average HTC calculated for the coarsest mesh is plotted against the number of elements. The number of prismatic elements has been kept constant for each mesh.

The extra-coarse and the coarse mesh show a noticeably different prediction of the HTC value while very little differences between the Mid, Fine and Extra-fine mesh are shown, reason why the mid mesh has been used in further analyses.

The flow path boundary conditions have been provided by BHGE, with reference to the FIGURE 2: a mass flow rate has been imposed as inlet boundary condition with a fixed ratio between tangential and axial components and 5% of turbulence intensity while an average static pressure value has been imposed as outlet boundary condition. In addition, a secondary inlet has been defined with the aim to simulate the leakage flow coming out from the previous stage. For each one of the geometries and the conditions tested the mass flow rate of the second inlet is assumed as 1% of the main one.

All the walls have been modelled as smooth and no-slip, therefore, a zero value of velocity has been assigned to the stationary walls while a rotating speed has been imposed to the rotating one. Moreover, since the heat transfer between fluid and wall structures has been calculated with an HTC-based approach, all the walls are isothermal with a fixed reduced temperature compared to steam inlet temperature to generate a temperature wall gradient allowing the calculation of a wall heat flux. This approach, widely used for forced convection problems, is based on the assumption of the HTC as invariant respect to the wall temperature and consequently, the HTC is as a scalable measure of convective heat transfer and fully determined by the fluid dynamics behaviour of the steam.

More specifically, referring to Newton's law:

$$\dot{q} = h\,(T_w - T_{aw}) \tag{1}$$

where q is the wall heat flux, h is the HTC, T_w is the fixed wall temperature and T_{aw} is the adiabatic wall temperature.

The equation (1) gives a linear dependence of $\dot{q}$ and T_w, and the calculation of h follows the solution of a linear system solved by the calculation of $\dot{q}$ at two specified wall temperature, this approach is called two-point method. Defining T_{w+} and T_{w-} the wall temperature imposed in the two CFD calculations and $\dot{q}_+$ and $\dot{q}_-$ the corresponding wall heat fluxes, the HTC is obtained with the following expression:

$$h = \frac{\dot{q}_+ - \dot{q}_-}{T_{w+} - T_{w-}} \tag{2}$$

The illustrated procedure is often implemented with a first CFD simulation with adiabatic wall, where wall heat flux is zero and the adiabatic wall temperature is mostly determined by the inlet temperature, with the exception of temperature variation dictated by fluid dynamics effect, and a second CFD simulation with isothermal walls with a fixed value of temperature obtained by a scaling respect to the adiabatic temperature. Neglecting the fluid dynamics effect is possible to assume the equality between the inlet and adiabatic temperature and consequently:

$$h = \frac{\dot{q}}{T_{in} - T_w} \tag{3}$$

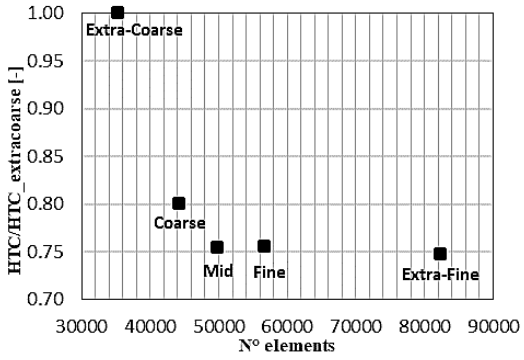

FIGURE 3 - Mesh sensitivity analysis.

An overview of the boundary conditions imposed for the design operating condition is reported in TABLE 2. Since the external diameter is directly linked to the overall sizing of the turbine the mass flow has been decreased (A > B > C > D) with external diameter to have the same axial velocity over the different cases. Also, the rotational speed has been varied with the external diameter (a > b > c > d) to keep constant the tangential velocity of the rotating wall and then the swirl ratio

The thermo-fluid dynamics conditions of the OP1 are representative of the feeding condition of the first steam chamber downstream of the impulse stage for the design operating condition.

To investigate the influence of thermodynamic and operating conditions additional 4 boundary conditions have been tested; OP2 and OP3 are representative of the steam thermodynamic conditions in two different axial locations in turbine flow path. The values of temperature and pressure have been chosen to match the conditions of the steam flowing in the last stages of the turbine. Since the operating condition is the same of OP1 the mass flow and the rotational speed have been kept constant for each external diameter. OP4 and OP5 are instead respectively representative of power idle and rotational speed idle operating conditions with reduced mass flow rate which are the most relevant conditions during start-up transient phases.

It is necessary to specify that for the OP3 an enlargement of the geometries, consistent with the real shape of the flow path, is required to decrease the needed values of the velocity at the inlet to maintain the same mass flow of OP1 and OP2 due to reduction in the density of the steam.

An overview of the boundary conditions imposed for all the conditions tested is reported in TABLE 3.

Considering the 64 geometries generated and the set of boundary conditions imposed, the total amount of numerical simulation is 320. Given this large number of simulations, only a 2 deg sector of the domain (quasi-2D) is

considered and rotational periodicity is used. This methodology, despite the need of some simplifications and assumptions to reduce the problem from 3D to quasi-2D, ensures less expensive simulations in terms of computational resources.

D [mm]	T [C°]	P [bar]	ω [rpm]	$\dot{m}$ [kg/s]	V_θ/V_x [-]
630	400	80	a	A	0.25
500	400	80	b	B	0.25
400	400	80	c	C	0.25
250	400	80	d	D	0.25

TABLE 2 - Boundary condition for the design operating condition

	T [C°]	P [bar]	ω [rpm]	$\dot{m}$ [kg/s]	V_θ/V_x [-]
OP1	400	80	a	A	0.25
OP2	350	30	a	A	0.25
OP3	170	3	a	A	0.25
OP4	350	5	b	B	-0.50
OP5	300	2	c	C	2

TABLE 3 - Boundary conditions for off-design operating conditions

A validation of this approach is reported in FIGURE 4 where a comparison of the velocity field obtained with the quasi-2D fluid domain and the full 3D one is reported. The comparison shows slight differences in the flow fields and therefore it is possible to conclude that the quasi-2D approach can offer a flow filed resolution quite similar compared to a 3D one.

In order to automatically perform the set of numerical simulation a convergence criterion is fundamental, in the present work the convergence of each simulation is verified checking the temperature calculated in a statistical monitor point located in the center of the chamber where a complex flow field is expected. Simulation convergence is achieved when the standard deviation of the temperature calculated in the last 250 iterations is below 0.001.

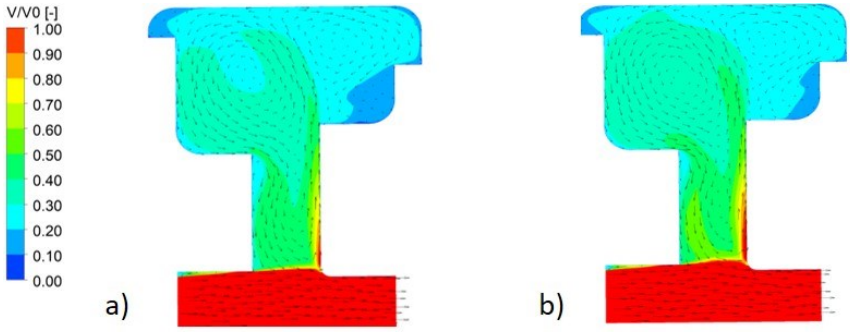

FIGURE 4 - Velocity distribution with quasi-2D approach (a) and full 3D (b).

NUMERICAL RESULTS

In this section, the results of the Design of Experiment analysis are reported. Although the heat transfer coefficients have been calculated on all surfaces of the domain only the results related to the casing surface are presented because is the surface object of the development of the numerical correlation. The results are presented in terms of non-dimensional heat transfer coefficient ($\hat{h}$), calculated as a ratio respect to the maximum HTC obtained in the present work. As a previous study have already reported [15-16], the axial length of the chamber (L1) have shown a weak impact on heat transfer coefficient, reason why in this section only the influence of L2 and D has been discussed.

Influence of Geometry

The influence of gap width on the flow field inside the chamber is illustrated in FIGURE 5. The strong influence of L2 on fluid dynamics behavior of the steam in the chamber is evident by observing the flow fields reported. In particular, the increase in gap width allows the onset of a counterclockwise in the middle of the chamber and a slower secondary clockwise vortex in the right of the chamber. These vortices enhance the convective heat transfer and therefore significantly increase the heat transfer coefficient with casing surface. Decreasing the gap width lead to a fluid dynamic behavior where the counterclockwise vortex is located in the upper part of the gap and a small secondary clockwise vortex flows in the chamber. In this case, given the presence of a single weak vortex, the heat transfer

coefficient is reduced in comparison with the previous case. Further, decreasing the gap width, the flow momentum in the gap is not able to induce a significant vortex in the chamber and heat transfer coefficient falls.

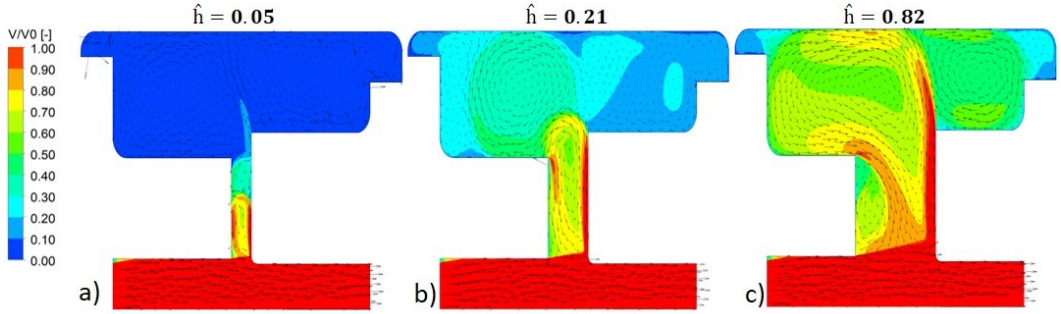

FIGURE 5 - Influence of gap width on the flow field: a) D=630 mm, L1= 600 mm, L2=37.5 mm; b) D=630 mm, L1= 600 mm, L2=75 mm; D=630 mm, L1= 600 mm, L2=150 mm. © 2019 Baker Hughes, a GE company, LLC - All rights reserved

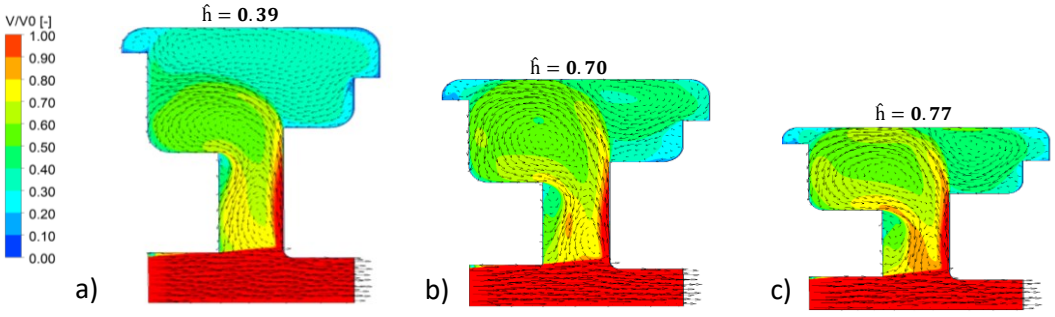

FIGURE 6 - Influence of external diameter on the flow field: a) D=500 mm, L1= 265 mm, L2=66.25 mm; b) D=400 mm, L1= 265 mm, L2=66.25 mm; D=250 mm, L1=265 mm, L2=66.25 mm. © 2019 Baker Hughes, a GE company, LLC - All rights reserved

A more comprehensive overview of the influence of the gap width on heat transfer coefficient is reported in FIGURE 7 where for each one of the widths of the chamber analyzed the no dimensional HTC values are reported as a function of L2 and D. The trends reported confirms that globally and increase in the gap width lead to increase in the heat transfer coefficient.

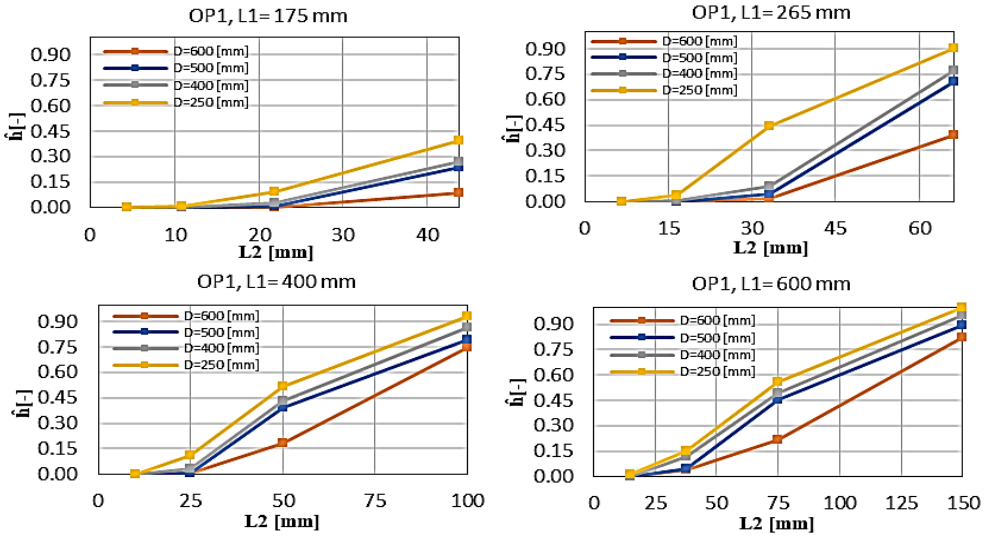

FIGURE 7 - Influence of gap width and external diameter on heat transfer coefficient. © 2019 Baker Hughes, a GE company, LLC - All rights reserved

Also the size of the turbine (D) has shown a strong impact on heat transfer coefficient, by referring to FIGURE 6 where the velocity fields for three different size of the chamber are shown, it is interesting to highlight as, despite the feeding condition of the chamber are quite similar, the fluid dynamic behavior of the steam in the chamber is markedly different only as a result of the radial size of the chamber. More specifically, for each geometry, the flow field in the chamber is dominated by the presence of two counterrotating vortexes, but for the geometries in FIGURE 6b and 6c, both the vortexes impinge on casing surface while for the geometry in FIGURE 6a only the clockwise one impinges on casing surface leading to a decrease in HTC. To summarize, the main effect of the radial size of the chamber is to bring the casing surface to the gap allowing the formation of a flow field like a jet impingement that enhances the convective heat transfer on the casing surface.

Another interesting finding, related to the radial size of chamber and probably due to the effect described above, is deductible by observing the FIGURE 7, the minimum gap width capable to induce a non-zero heat transfer coefficient on casing is influenced by the size of the steam turbine.

Influence of Thermodynamic and Operating Condition

FIGURE 8 shows the velocity contours for the OP1, OP2 and OP3. Despite the flow fields are quite similar, except for the velocity magnitude, significant variations of the heat transfer coefficient have been observed. The main reason for the fall in the heat transfer coefficient for the OP2 and OP3 is the changing in thermal properties of the steam due to the variation in temperature and pressure. The rise of the velocity magnitude for the OP2 and OP3, which should increase the convective heat transfer, is not such as to compensate the effect described above.

Finally, the effect of off-design operating conditions on heat transfer phenomena in the chamber has been evaluated. FIGURE 9 indicates that in reduced power off-design condition no difference respect to OP1 in the flow filed are detected and consequently the falls down in the heat transfer coefficients is again a direct consequence of the different thermal properties of the steam, while in the reduced rotational speed condition the mass flow reduction does not allow the onset of the vortices in the chamber, reason why this operating condition is characterized by the lowest value of HTC.

These findings are mostly confirmed also by the graph reported in FIGURE 10, where, for a fixed D and L1, the no-dimensional HTC to varying of L2 is reported for each OP tested.

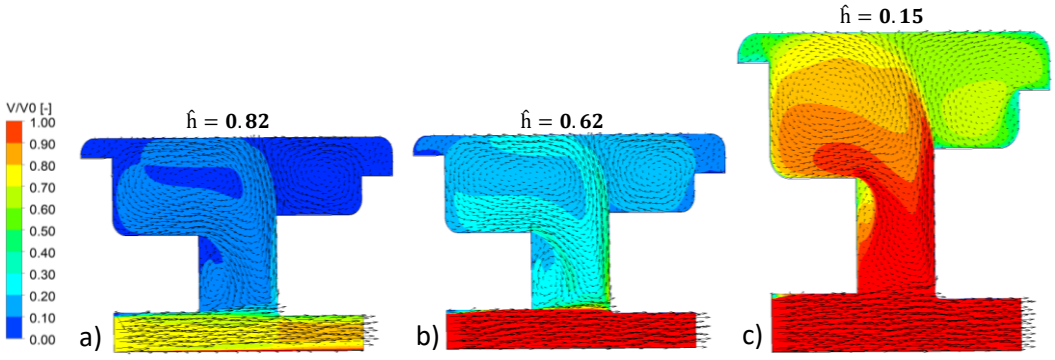

FIGURE 8 - Influence of thermodynamic conditions: a) OP1; b) OP2; c) OP3.

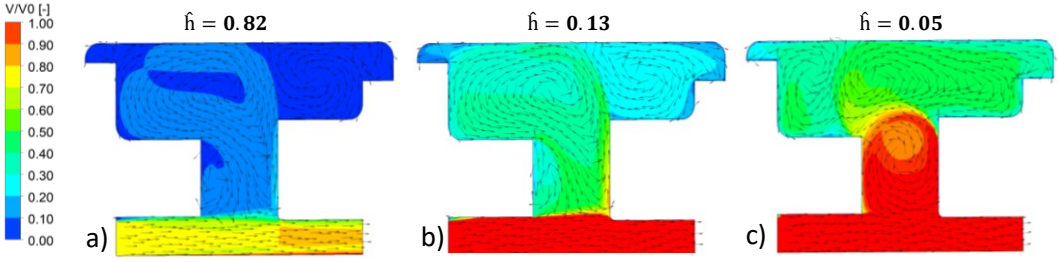

FIGURE 9 - Influence of operating conditions: a) OP1; b) OP4; c) OP5.

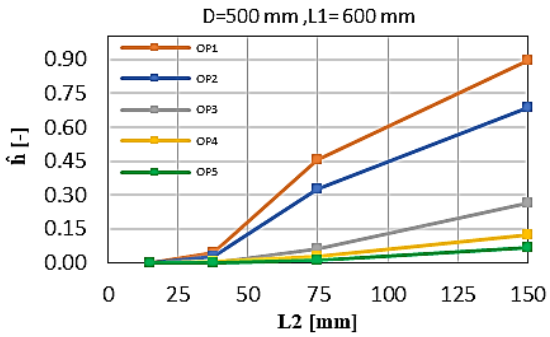

FIGURE 10 - Influence of thermodynamic and operating conditions.

DEVELOPMENT OF NUMERICAL CORRELATION

In this section, the methodology followed to develop a numerical correlation to determine the heat transfer coefficient on casing surface for different chamber geometry and in different operating condition is reported.
As first step, a dimensionless parameter L* has been defined, which considers all the effect dependent on shape and dimension of the chamber:

$$L^* = f\,(D, L1, L2) \tag{4}$$

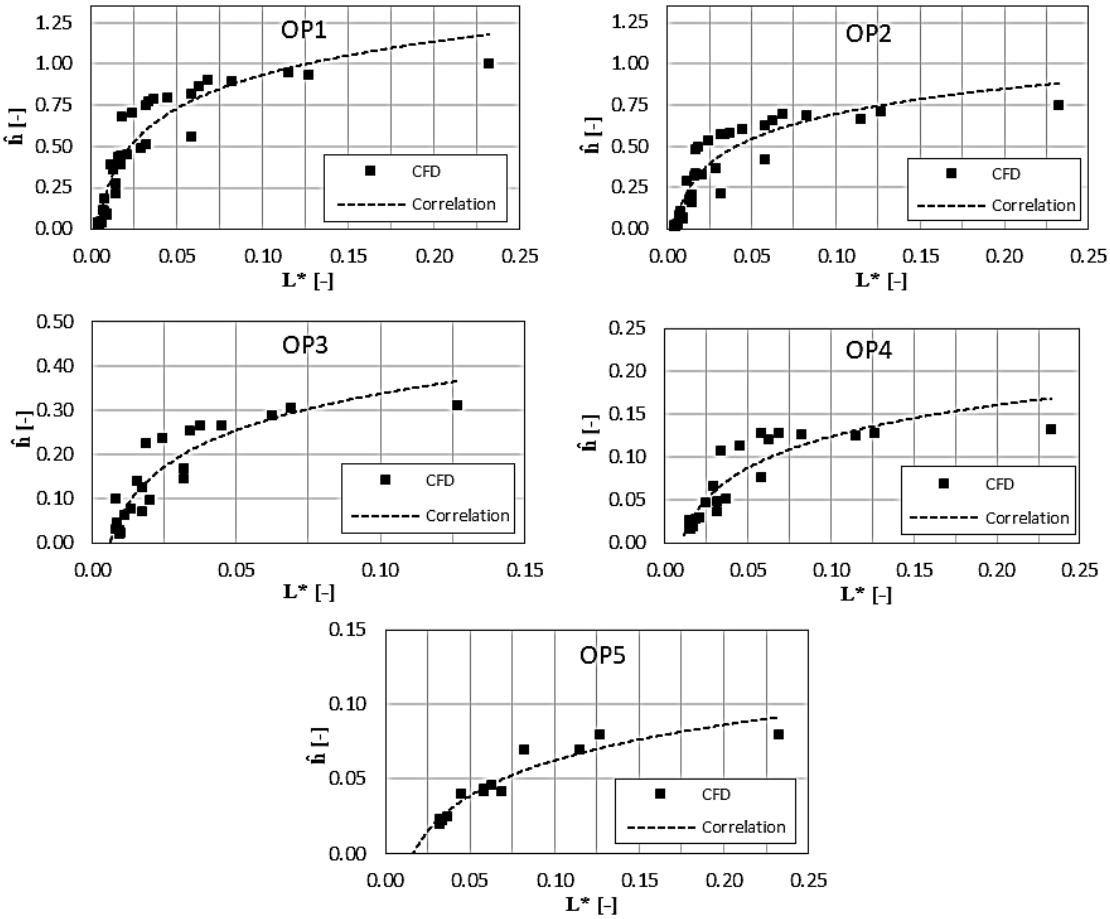

FIGURE 11 - ĥ as a function of L*.

As illustrated in the results section, some of the steam chamber tested have shown values of heat transfer close to zero, since these geometries do not provide any useful additional information for the development of the correlation they have been excluded in the following step by the definition of a critical value of L* below which the correlation returns a minimum constant value of heat transfer coefficient.
As shown in FIGURE 11, L* allows the definition of a correlation that can describe with quite successfully accuracy the trend of the heat transfer coefficient for almost all the simulated feeding condition of the chamber. It is interesting to underline as the logarithmic shape of the fitting curve is the same for all the condition. The HTC can, therefore, be defined as:

$$h = A\log(L^*) + B \tag{5}$$

Where A and B are coefficients dependent on thermodynamic and operating conditions. This dependency has been quantified in terms of temperature, pressure and mass flow:

$$A = f_1(T, P, \dot{m});\ B = f_2(T, P, \dot{m}) \tag{6}$$

To evaluate the overall quality of the fitting process, the heat transfer coefficients predicted with the developed correlation have been plotted against the CFD results. Such a plot, illustrated in FIGURE 12, shows as the correlation can reproduce reasonably well the CFD predictions.

As a final step, a validation of the correlation has been carried out through the definition of a new off-design operating point (OP6). The boundary condition imposed in this condition are reported in TABLE 4. The FIGURE 13 highlights that the correlation can predict very well the heat transfer coefficients for this new operating condition.

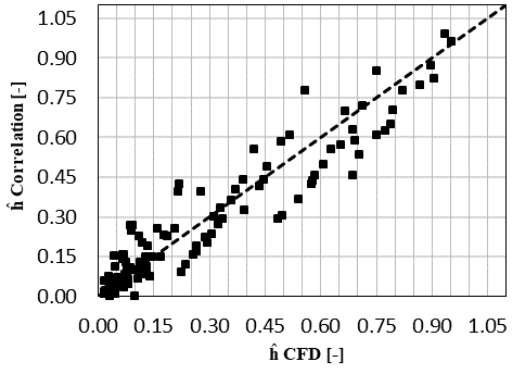

FIGURE 12 - Comparison between the prediction of the correlation and the CFD results. © 2019 Baker Hughes, a GE company, LLC - All rights reserved

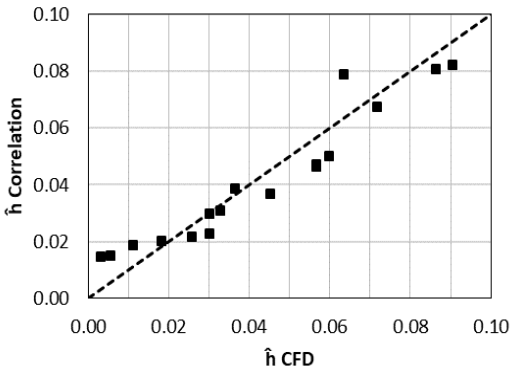

FIGURE 13 - Comparison between the prediction of the correlation and the CFD results for the OP6. © 2019 Baker Hughes, a GE company, LLC - All rights reserved

	T [C°]	P [bar]	ω [rpm]	$\dot{m}$ [kg/s]	V_θ/V_x [-]
OP6	325	3.5	a	D	0.75

TABLE 4 – Boundary conditions for OP6

CONCLUSIONS

The knowledge of flow and heat transfer phenomena steam turbine cavities is a fundamental issue to estimate with sufficient accuracy heat transfer coefficient between steam and wall structures of the cavity to be used as thermal boundary for detailed FEM simulations. This work aims to contribute to this topic with the implantation of a Design of Experiment, based on computational fluid dynamic simulations and focused on the investigation on the cavity geometry impact and of the steam thermodynamic condition on heat transfer coefficient with the upper wall of the cavity. The results of the numerical simulations have been post-processed to determine a numerical correlation for the heat transfer coefficient calculation applicable for different cavities and under different operating condition. The present correlation, although obtained with several assumptions, could still be included in the design practice of the steam turbine and could provide the starting for further development of the correlation which considers additional parameters in order to increase the overall accuracy and flexibility.

ACKNOWLEDGMENTS

This work has been carried out in the framework of the research program Smart Turbine Technologies (STECH Bando FAR-FAS 2014, CUP -ST-4421.02102014.072000044) among Regione Toscana and Nuovo Pignone Tecnologie srl within objective number six. The authors would like to thank for the fundamental contribution the Programma Attuativo Regionale, co-funded by FAS. Further, the authors would like to gratefully acknowledge Lorenzo Winchler for his contribution.

REFERENCES

[1] W. Aung, A. Bhatti, Finite difference analysis of laminar separated forced convection in cavities. Journal of Heat Transfer 106 (1) (1984) 49–54.

[2] R.F. Richards, M.F. Young, J.C. Haiad, turbulent forced convection heat transfer from a bottom heated open surface cavity. International Journal of Heat Mass Transfer 30 (1987) 2281–2287.

[3] D.E. Metzger, R.S. Bunker, M.K. Chyu, Cavity heat transfer on a transverse grooved wall in a narrow flow channel. Journal of Heat Transfer 111 (1) (1989) 73–79.

[4] A. Ooi, G. Iaccarino, M. Behnia, Heat Transfer Predictions in Cavities, Annual Research Briefs. Center for Turbulence Research, NASA Ames/Stanford Univ., 1998, pp. 185–196.

[5] P.S.D. Zdanski, M.A. Ortega, G.C.R. Nide, Fico, Jr., Numerical simulations of turbulent flows over shallow cavities, in: Proceedings of the 2nd Int. Conference on Computational Heat and Mass Transfer, 2001, Oct. 22–26.

[6] P.S.B. Zdanski, M.A. Ortega, G.C.R. Nide, Fico Jr., Numerical study of the flow over shallow cavities. Computer and Fluids 32 (2003) 953–974.

[7] D.H. Lee, J.S. Lee, H.J. Park, M.K. Kim, Experimental and numerical study of heat transfer downstream of an axisymmetric abrupt expansion and in a cavity of a circular tube, J. Mech. Sci. Technol. 25 (2011) 395e401.

[8] H. Yamamoto, N. Seki, S. Fukusako, Forced convection heat transfer on a heated bottom surface of cavity with different wall-height, Waķrme Stoffü- bertragung 17 (1983) 73e83.

[9] D.E. Metzger, R.S. Bunker, M.K. Chyu, Cavity heat transfer on a transverse grooved Wall in a narrow flow channel, J. Heat Transfer 111 (1989) 73e79.

[10] R.L. Haugen, A.M. Dhanak, Heat transfer in turbulent boundary layer separation over a surface cavity, J. Heat Transfer 89 (1967) 335e340.

[11] M. Yoshiwara, Convective Heat Transfer from the Wall Surface of a Cavity to the external Stream, JSME International Journal, Vol. 44, No.2 262-273 (2001)

[12] A. Aroussi, I. Grant, Y.-Y. Yan, E. Owen, A comparison between LDA and PIV measurements and numerical predictions of the flow in an L-shaped cavity, in: A. Dybbs, B. Ghorashi (Eds.), Laser Anemometry e Advances and Appli- cations, 1991, pp. 267e272

[13] A. Aroussi, Y.-Y. Yan, I. Grant, Experimental verification of numerical simulation of turbulent flow past enclosures in offshore structures, Opt. Laser. Eng. 16 (1992) 391e409

[14] A. Aroussi, Measurement and prediction of recirculating flows in a 'T' shaped cavity, in: G. de Vahl Davis, C. Fletcher (Eds.), Computational Fluid Dynamics, 1988, pp. 229e237

[15] D.Spura, J.Lueckert,S.Schoene,U. Gampe, Concept development for the experimental investigation of forced convection hea transfer in circumferential cavities with variable geometry, International Journal of Thermal Sciences 96 (2015) 277-289.

[16] D.Spura, U.Gampe, G. Eschmann, W.Uffrecht, Experimental investigation of heat transfer in cavities of steam turbine casings under generic test rig conditions, ASME Proceedings, Paper No. GT2018-75463.

[17] Menter, F., "Two-Equation Eddy-Viscosity Turbulence Models for Engineering Applications," AIAA Journal, Vol. 32, No. 8, 1994, pp. 1598–1605.